ESI (Electronic Supplementary Information)

Title:

Elucidation of the reaction mechanism on dry reforming of methane in an electric field by *in-situ* DRIFTs

Authors

Naoya Nakano[a], Maki Torimoto[a], Hiroshi Sampei[a], Reiji Yamashita[a], Ryota Yamano[a], Koki Saegusa[a], Ayaka Motomura[a], Kaho Nagakawa[a], Hideaki Tsuneki[a], Shuhei Ogo[b,c] and Yasushi Sekine[*a]

a Department of Applied Chemistry, Waseda University, 3-4-1, Okubo, Shinjuku, Tokyo, 169-8555, Japan, E-mail ysekine@waseda.jp, +81-3-5286-3114

b Department of Marine Resources Science, Faculty of Agriculture and Marine Science, Kochi University, Nankoku, 783-8502, Japan

c Center for Advanced Marine Core Research, Kochi University, Nankoku, 783-8502, Japan

1. Reaction apparatus

For the evaluation of catalytic activities of Pt/CeO_2 catalyst, we used an apparatus as shown in Figure S1.

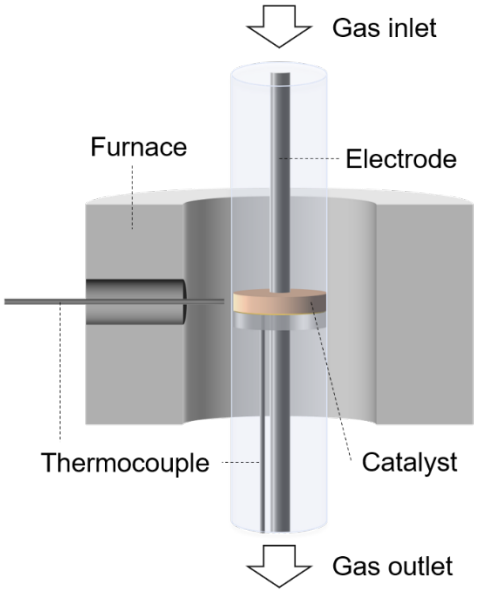

Figure S1. A schematic image of the apparatus for activity tests.

2. Calculation

The conversion, yield, and input power were calculated by the following equations. In these equations, *F* denotes the product formation rate, *S* denotes the supply rate of the reactant, and r_{DR} and r_{RWGS} respectively represent the reaction rates of DR and RWGS reactions.

$$r_{DR}=\frac{F_{H2}+F_{CO}}{4} \quad 2.1$$

$$r_{RWGS}=\frac{F_{CO}-F_{H2}}{2} \quad 2.2$$

$$CH_4 \text{ conv. } (\%)=\frac{r_{DR}}{S_{CH4}}\times 100 \quad 2.3$$

$$CO_2 \text{ conv. } (\%)=\frac{r_{DR}+r_{RWGS}}{S_{CO2}}\times 100 \quad 2.4$$

$$\text{CO yield (\%)} = \frac{\text{CH}_4 \text{ conv.} \times \text{CO sel.}}{100} \quad (2.5)$$

$$\text{Input power (W)} = \text{Input current (mA)} \times \text{Applied voltage (kV)} \quad (2.6)$$

$$\text{Power efficiency(-)} = \frac{\text{Endothermic enthalpy in reaction (J s}^{-1}\text{)}}{\text{Input power (W)}} \quad (2.7)$$

The Ce^{3+} fraction was calculated by the following equation.

$$Ce^{3+} \text{ fraction (\%)} = \frac{Ce^{3+}}{Ce^{3+}+Ce^{4+}} \times 100 \quad (2.8)$$

3 *in–situ* DRIFTS assignments

Table S1. Assignments of vibrational bands in the DRIFT spectra at various CeO_2 based catalysts.

Structure	Band / cm^{-1}	Peak position / cm^{-1}
monodentate carbonate 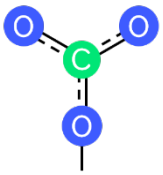	1085-1088	(1085)[58], (1088)[68]
	1160	(1160)[69]
	1252	(1252)[68]
	1333-1352	(1333)[70], (1344)[71], (1348)[58], (1348)[72], (1349)[73], (1351)[74], (1351)[48], (1352)[68]
	1357-1360	(1357)[49], (1358)[58], (1360)[50]
	1399-1404	(1399)[70], (1402)[51], (1400, 1404)[52]
	1442-1460	(1442)[73], (1454)[72], (1460)[53]
	1463-1472	(1463)[54], (1464)[58], (1465)[48], (1467)[68], (1472)[70]
	1489	(1489)[55]
	1504-1519	(1504)[71], (1504)[74], (1504)[48], (1507)[56], (1509)[57], (1510)[49], (1510)[50], (1519)[59], (1505, 1514)[70]
	1527	(1527)[73]
	1540	(1540)[57]

	1578-1580	(1578)[52], (1580)[50], (1580)[51]
bidentate carbonate	1009-1024	(1011)[68], (1011)[72], (1011)[56], (1014)[74], (1021)[48], (1024)[52], (1009-1014)[58]
	1028-1034	(1028)[58], (1028)[72], (1030)[52], (1032)[53]
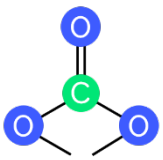	1265-1273	(1266)[60], (1273)[61], (1265, 1267)[52]
	1281-1303	(1286)[72], (1287)[56], (1289)[74], (1289)[62], (1289)[63], (1290)[48], (1290)[53], (1292)[51], (1292)[54], (1292)[59], (1294)[71], (1298)[58], (1300)[50], (1300)[60], (1281, 1298)[52], (1290, 1301)[70], (1298, 1303)[57]
	1315	(1315)[50]
	1541	(1541)[73]
	1560-1576	(1560)[68], (1562)[61], (1567)[74], (1568)[57], (1570)[71], (1570)[56], (1570)[11], (1572)[52], (1574)[70], (1575)[53], (1575)[59], (1576)[48], (1562, 1565)[58], (1562, 1568)[72]
	1580-1581	(1580)[51], (1580)[54], (1580)[60], (1581)[70]
	1647	(1647)[52]
bridged carbonate	1120-1150	(1120)[48], (1132)[72], (1135)[74], (1150)[61], (1122, 1124)[52], (1132, 1145)[58]
	1195	(1195)[49]
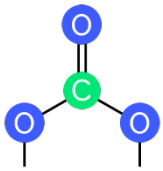	1208	(1208)[52]
	1232-1242	(1232)[58], (1241)[51], (1242)[54]
	1651	(1651)[54]
	1675-1695	(1675, 1687)[51], (1688, 1695)[52]
	1728-1740	(1728)[72], (1736)[74], (1736)[48], (1728, 1740)[58]
	1781	(1781)[52]
polydentate carbonate	1066-1074	(1066)[58], (1066)[74], (1073)[62]
	1352-1353	(1352)[62], (1353)[58], (1353)[74]
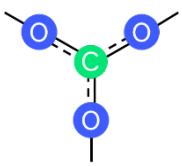	1366-1389	(1366)[71], (1367)[56], (1373)[62], (1376)[11], (1378)[59], (1389)[5]
	1462	(1462)[58], (1462)[71], (1462)[74]
	1473-1479	(1473)[62], (1476)[56], (1479)[59]
	1591	(1591)[57]

bicarbonate 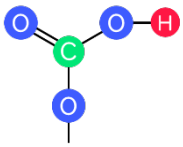	990	(990)[64]
	1025	(1025)[74], (1025)[48], (1025)[51]
	1043-1060	(1045)[74], (1056)[52], (1060)[59], (1043, 1045)[58]
	1210-1220	(1212)[48], (1212)[65], (1214)[50], (1215)[54], (1216)[52], (1216)[60], (1217)[71], (1217)[56], (1218)[74], (1220)[69], (1220)[59], (1220)[61], (1215, 1216)[51], (1217, 1218)[58], (1217, 1220)[70]
	1390-1398	(1390)[64], (1390)[65], (1391)[74], (1392)[74], (1396)[71], (1398)[54], (1391, 1393)[58], (1392, 1395)[52]
	1404-1436	(1404)[56], (1405)[50], (1413)[68], (1413)[74], (1413)[48], (1419)[71], (1411, 1415)[70], (1436, 1425-1426)[49]
	1590-1616	(1590)[65], (1594)[59], (1598)[68], (1599)[48], (1600)[54], (1600)[60], (1603)[61], (1608)[71], (1609)[51], (1614)[50], (1599, 1613)[74], (1603, 1608)[70], (1609, 1615)[57], (1611, 1613)[58], (1611, 1616)[52]
	1641	(1641-1642)[49]
formate 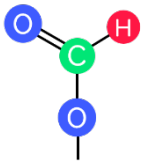	1329-1330	(1329)[66], (1330)[67], (1329, 1330)[58]
	1353-1355	(1353)[68], (1354)[54], (1355)[67]
	1368-1372	(1368)[59], (1369)[72], (1369)[66], (1370)[65], (1371)[68], (1371)[54], (1372)[58]
	1545-1558	(1545)[61], (1550)[65], (1555)[53], (1555)[67], (1557)[68], (1558)[72], (1558)[62], (1558)[66]
	1582-1587	(1585)[65], (1582, 1587)[58]

4. Prepared catalysts

Following figures show the nature of prepared catalyst of Pt/CeO_2.

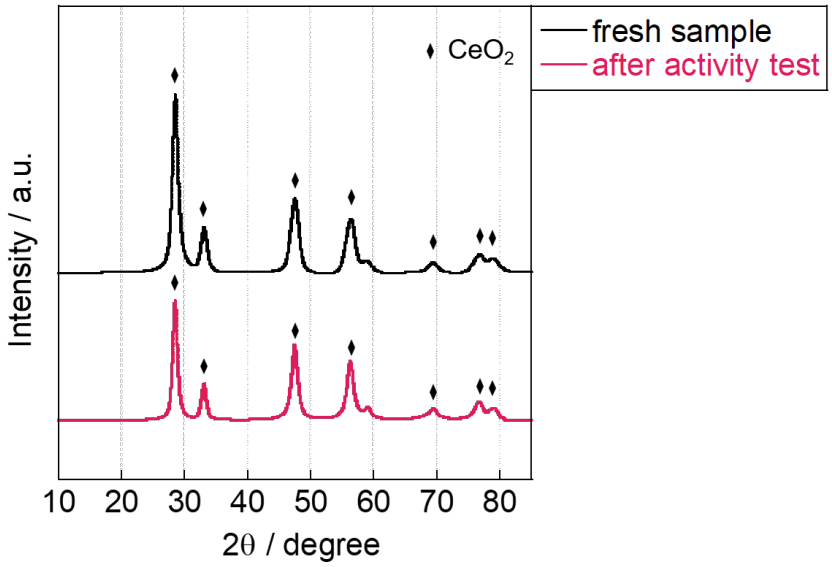

Figure S2. XRD patterns of 1 wt% Pt/CeO_2 (fresh and after activity test).

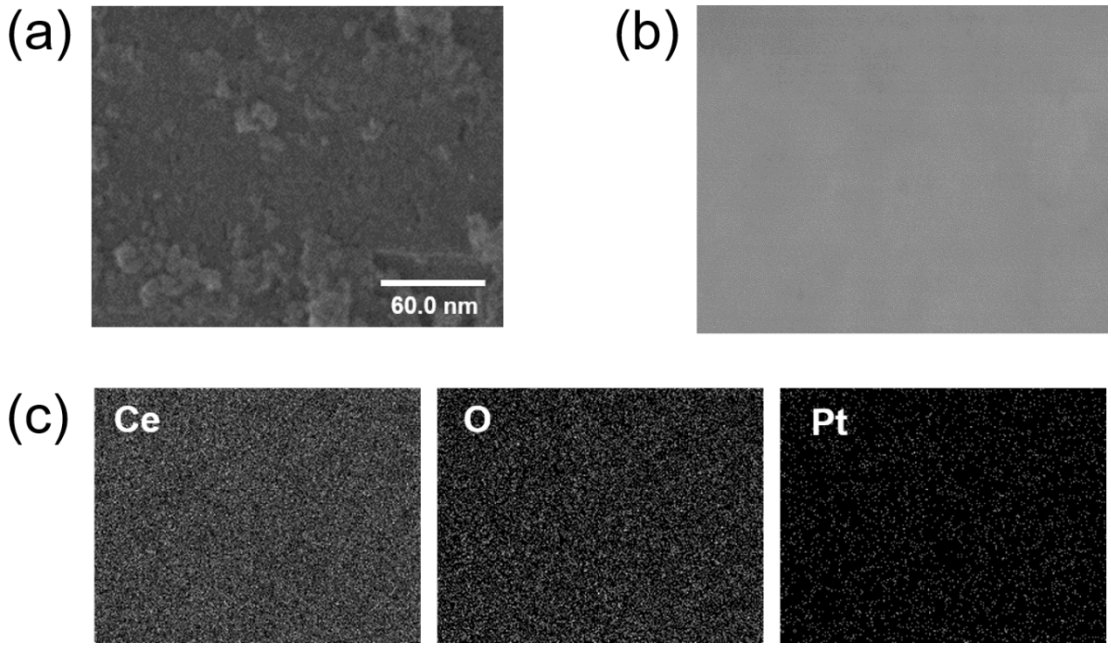

Figure S3. HAADF-STEM images of fresh 1 wt% Pt/CeO_2, (a) STEM image (b) HAADF-STEM image (c) EDX elemental mappings of Ce, O, Pt.

5. Catalytic activities and other results

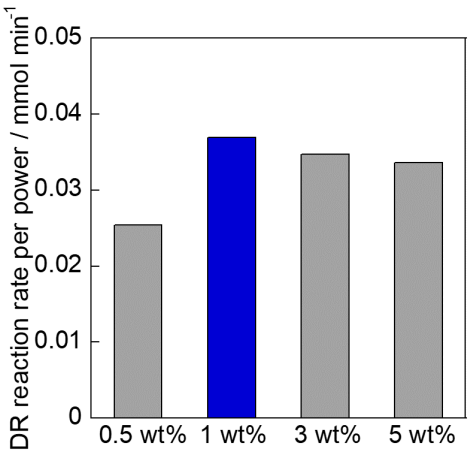

Figure S4. Reaction rate over various catalysts. Reaction conditions: 0.1 g of Pt/CeO_2; CH_4: CO_2: Ar = 1:1:2, total 80 SCCM; reaction temperature was 473 K; 10 mA imposed current.

Table S2. Catalytic activity over 1wt% Pt/CeO_2 with, without EF; CH_4: CO_2: Ar = 1:1:2; 80 SCCM total flow rate; 300 mg catalyst weight; 20.0 mA imposed current.

Temp. / K	CH_4 conv. / %	CO_2 conv. / %	H_2/CO / -	Input current / mA	Voltage / V	Power / W	Faradaic number / -	Energy efficiency / -	Field intensity / V mm^{-1}
453	15.1	16.4	0.763	20.0	140	2.81	14.5	0.186	57.3
473	15.0	16.5	0.754	20.0	145	2.91	14.5	0.179	59.3
523	15.9	17.9	0.728	20.0	137	2.74	15.5	0.203	56.0
573	16.4	19.2	0.696	20.0	130	2.61	16.4	0.223	53.2
623	17.4	20.9	0.667	20.0	127	2.54	17.7	0.244	51.8
672	19.1	24.0	0.625	20.0	132	2.63	20.0	0.262	53.8
723	27.5	34.6	0.623	20.0	144	2.87	28.8	0.347	58.6
472	0	0	-	-	-	-	-	-	-
523	0.00	0.01	0.00	-	-	-	-	-	-
573	0.03	0.07	0.00	-	-	-	-	-	-
623	0.15	0.42	0.00	-	-	-	-	-	-
673	0.66	1.60	0.135	-	-	-	-	-	-
723	2.21	4.75	0.237	-	-	-	-	-	-

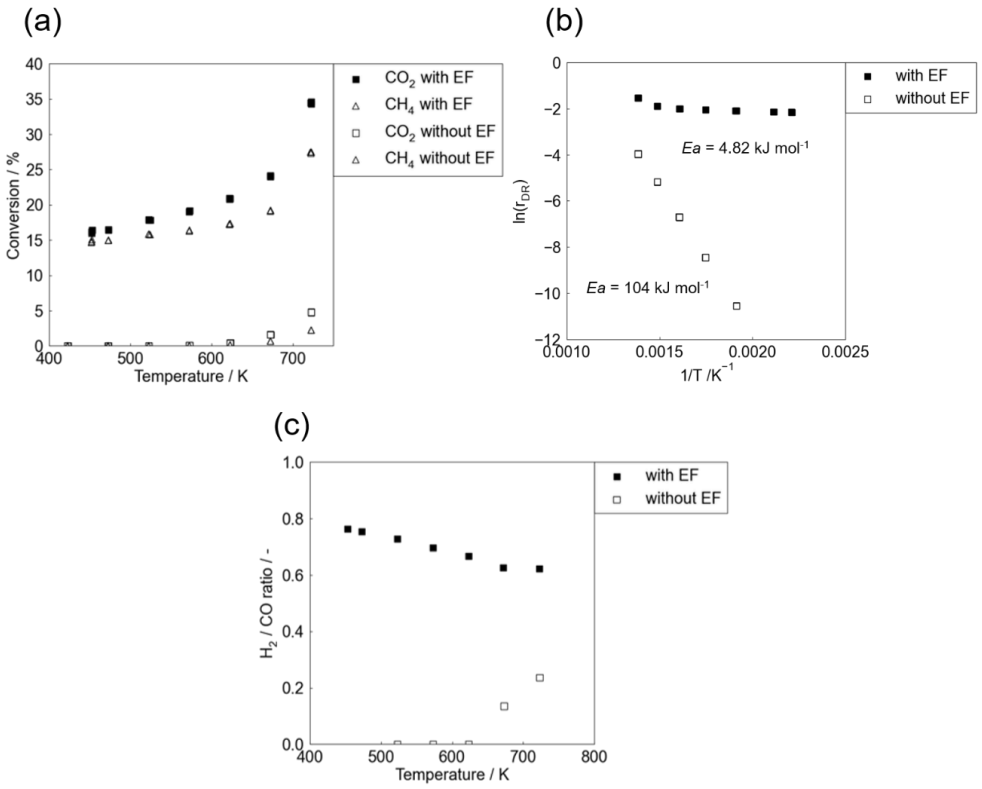

Figure S5. (a) Comparison of the conversion with, without EF over 1wt% Pt/CeO_2 (b) Arrhenius plot of DRM reaction rate, (c) H_2/CO ratio with, without EF; CH_4: CO_2: Ar = 1: 1: 2; 80 SCCM total flow rate; 300 mg catalyst weight; 20.0 mA imposed current.

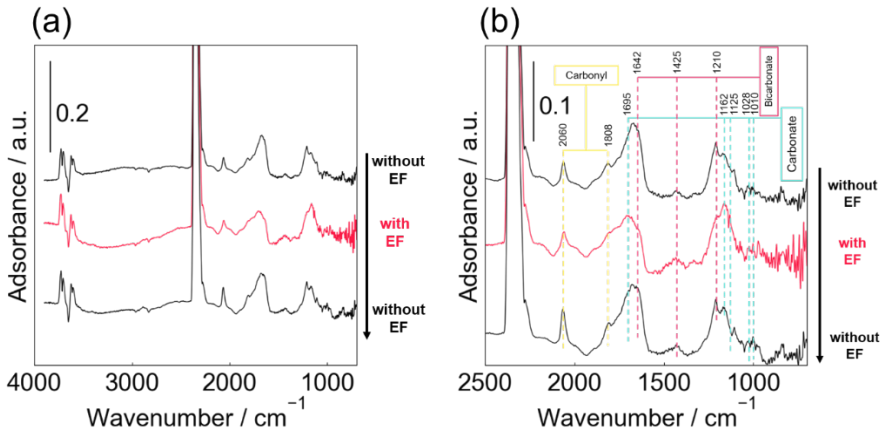

Figure S6. *In-situ* DRIFT spectra after switching the EF on and off and hold 20 min at 473 K over 1wt% Pt/CeO_2; Ar: CO_2 = 8: 1, total 90 SCCM; 3 mA imposed current; (a) spectra in 700 – 4000 cm^{-1}, (b) spectra in 700 – 2300 cm^{-1} region.

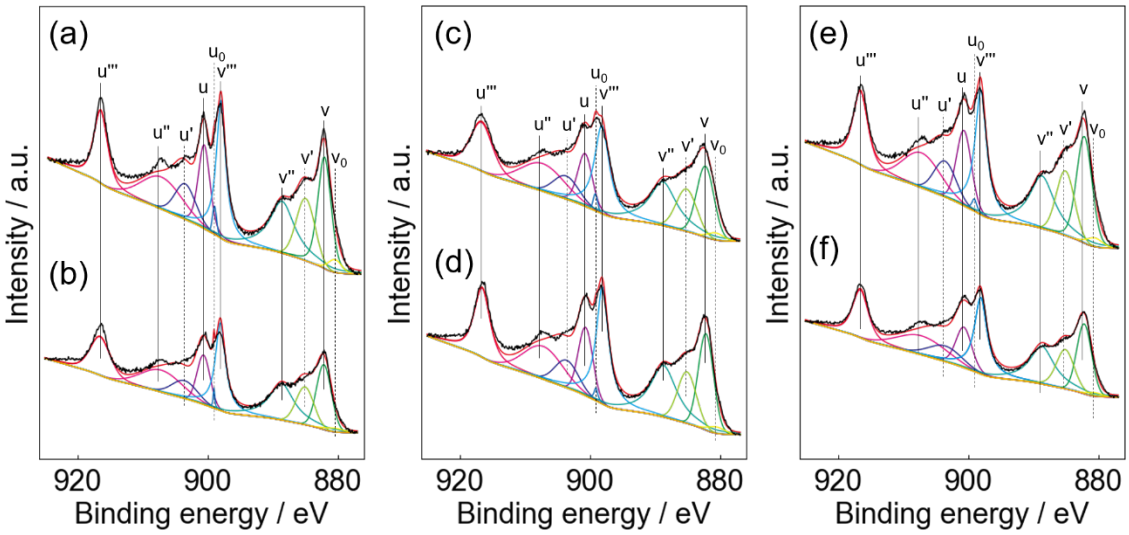

Figure S7. XPS spectra of 1wt% Pt/CeO_2 under CH_4 flow(left) with (a), without (b) EF, under Ar flow (middle) with (c), without(d) EF, under CO_2 flow(right) with (e), without (d) EF.

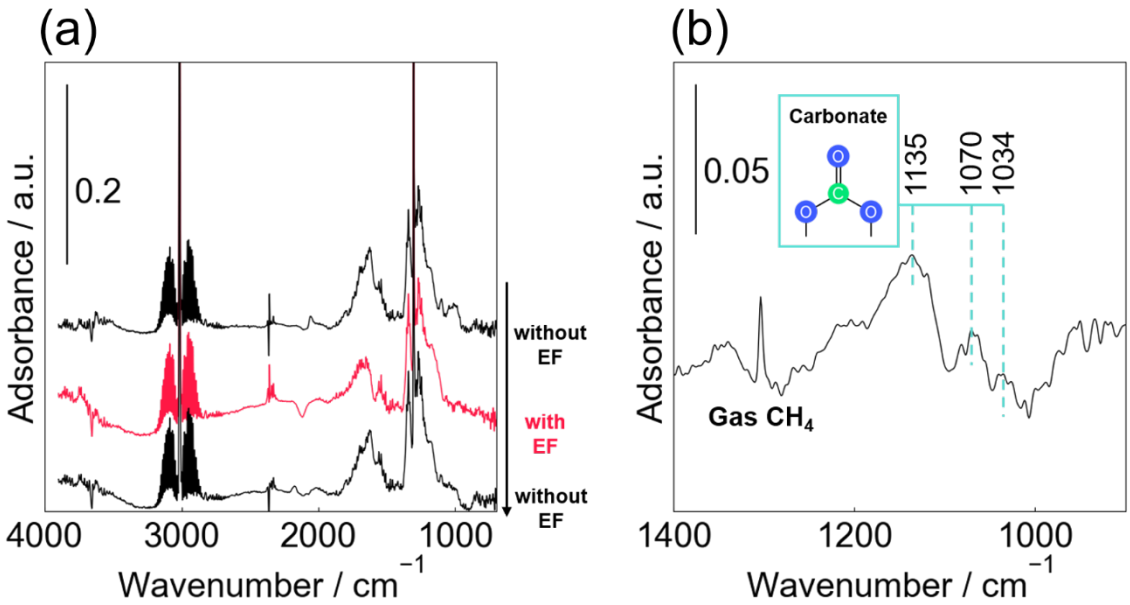

Figure S8. (a) Comparison of DRIFT spectra over 1wt% Pt/CeO_2 with, without EF in CH_4 flow, (b) difference spectrum in 900 – 1400 cm^{-1} region (with EF – without EF); Ar: CO_2 = 8: 1, total 90 SCCM; 3 mA imposed current.

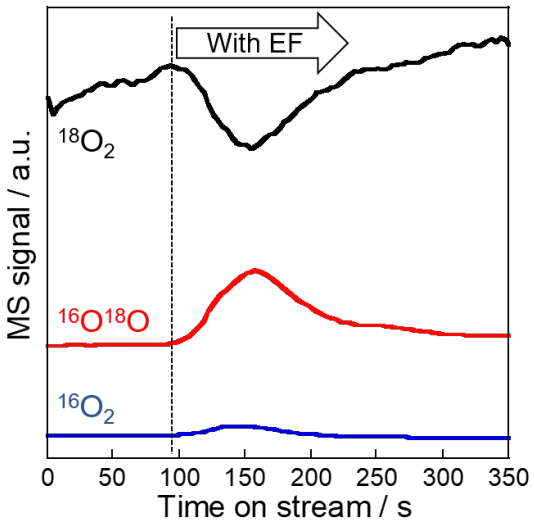

Figure S9. Formation rates of various gas productions in 2500 ppm $^{18}O_2$ (2500 ppm; 100 SCCM total flow rate) over 0.5wt% Pd supported $Ce_{0.7}Zr_{0.3}{}^{16}O_2$ catalyst at 373 K.

Isotopic exchange test was conducted by following procedure.

Isotopic exchange test was conducted using a quadrupole mass spectrometer (Q-Mass, QGA; Hiden Analytical Ltd.) with 0.5 wt% $Pd/Ce_{0.7}Zr_{0.3}O_2$. The catalysts were pre-oxidized and reduced at 773 K for 15 min, respectively. The oxidation gas was 5% $^{16}O_2$, and the reduction gas was 5 % H_2. After the pre-treatment, the catalyst was parged with Ar at 373 K. We applied the EF in the 50 % $^{18}O_2$ flow and analyzed the production gas. All the gases were diluted to 100 SCCM with Ar.

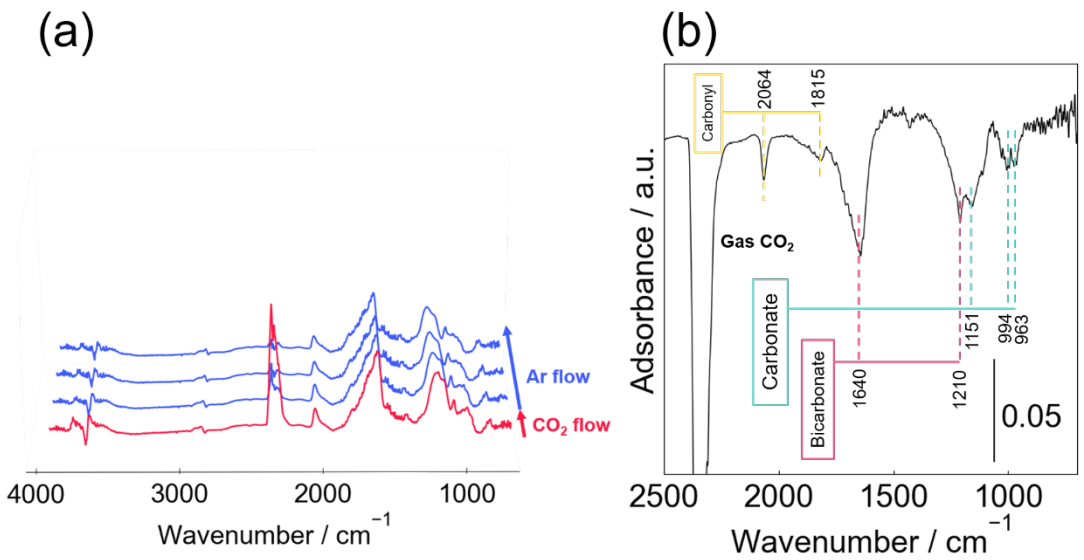

Figure S10. *In-situ* DRIFT spectra over 1wt% Pt/CeO_2 at 473 K after switching CO_2 (Ar: CO_2 = 8: 1, 90 SCCM total flow rate) to Ar (Ar; 90 SCCM total flow rate) feeds and hold 20 min at 473 K; 3 mA imposed current. (a) spectra in 700 – 4000 cm^{-1}, (b) differential spectra in 700 – 2500 cm^{-1} (Ar – CO_2).

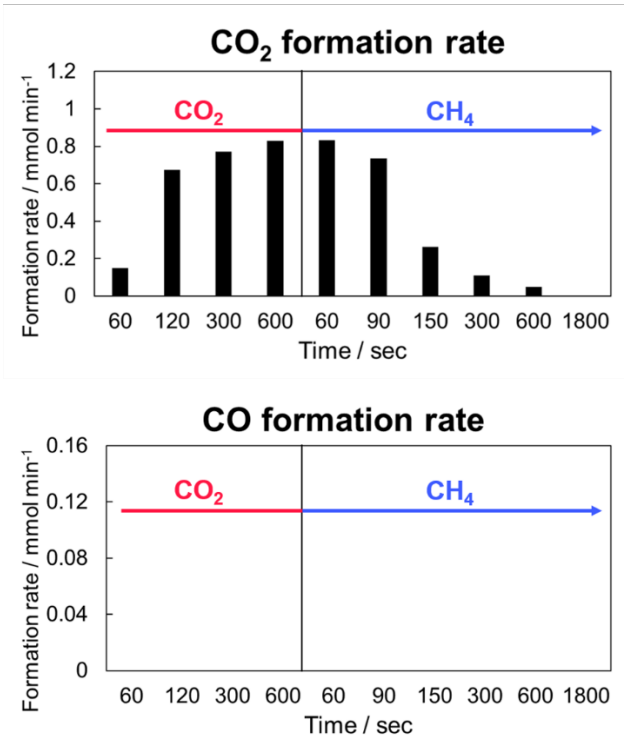

Figure S11. CO_2 and CO formation rate over 1wt% Pt/CeO_2 without EF before and after switching CO_2 (CO_2: Ar = 8: 1, 90 SCCM total flow rate) to Ar (Ar 80 SCCM total flow rate) flow at 473 K.

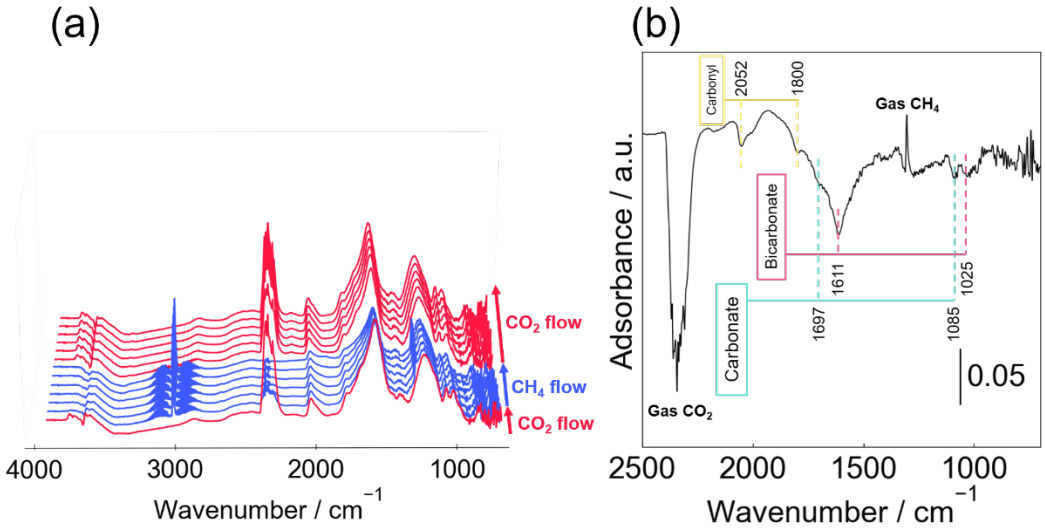

Figure S12. *In-situ* DRIFT spectra over 1wt% Pt/CeO_2 switching between CO_2 (CO_2: Ar = 1: 8; 90 SCCM total flow rate) and CH_4 (CH_4: Ar = 1: 8; 90 SCCM total flow rate) feeds at 473 K; (a) 60, 120, 180, 300, 600, 1200 seconds after switching to CH_4, 60, 120, 180, 300, 600, 1200 seconds after switching to CO_2, (b) differential spectra of steady state in 700 – 2500 cm^{-1} (CH_4 – CO_2).

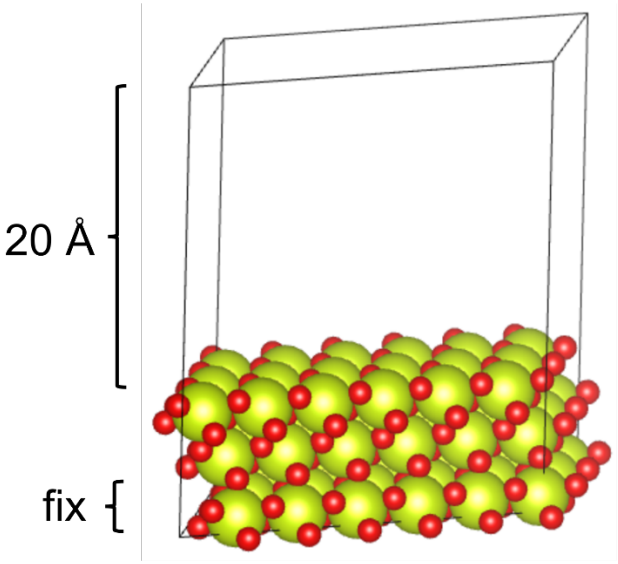

Figure S13. The CeO_2 slab model, the yellow green, and red sphere are Ce, O, respectively.

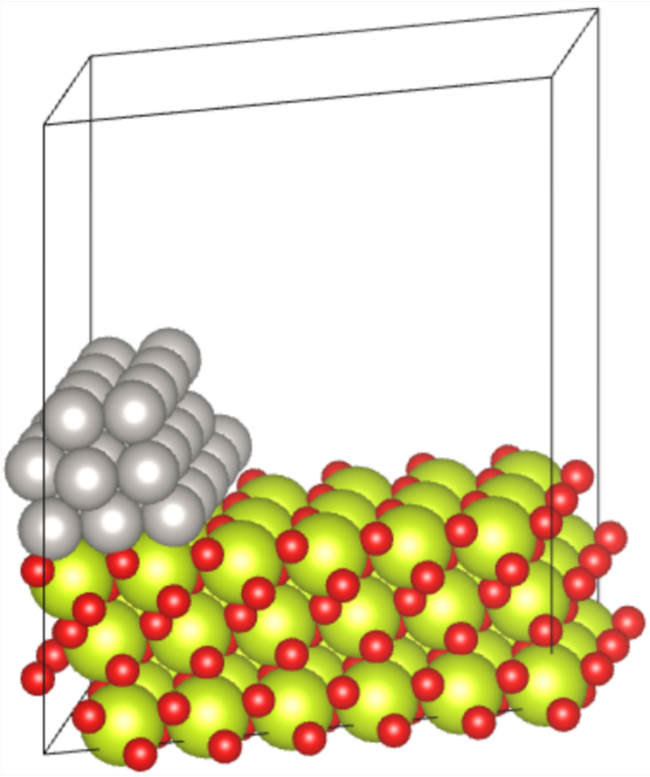

Figure S14. The Pt/CeO_2 model, the yellow green, red, and silver sphere are Ce, O, and Pt, respectively.

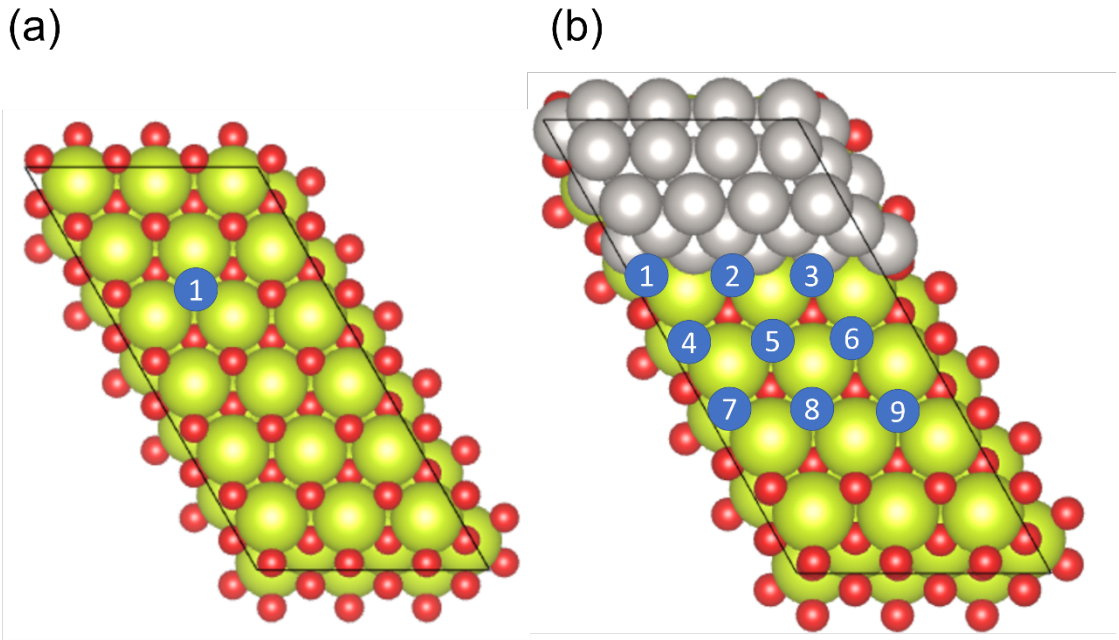

Figure S15. The calculated oxygen defect locations; (a)CeO_2, (b)Pt/CeO_2.

Table S3. The formation energy of oxygen defect (V_{ox}) at each site.

model	Vox site	E(Vox) / eV
CeO_2	1	4.148
Pt/CeO_2	1	3.994
	2	3.790
	3	3.997
	4	4.825
	5	4.803
	6	4.861
	7	4.876
	8	4.853
	9	4.875